2007 IEEE International Conference on
Robotics and Automation
Roma, Italy, 10-14 April 2007

Dynamic Trajectory Generation for Spatially Constrained Mechanical Systems Using Harmonic Potential Fields

Ahmad A. Masoud
Electrical Engineering Department, KFUPM, P.O. Box 287, Dhaharan 31261, Saudi Arabia, masoud@kfupm.edu.sa

Abstract- The harmonic potential field (HPF) approach to motion planning is shown to provide an efficient and provably-correct basis for building intelligent, context-sensitive, and goal-oriented controllers. In [1] a novel type of dampening forces called: nonlinear, anisotropic, dampening forces (NADFs) are used to convert the guidance signal from an HPF into a navigation control signal with verifiable capabilities. This work provides two extensions of the NADF approach. The first is a blind, iterative procedure that can totally cancel the steady state error. The other extension is concerned with the nonholonomic case. Theoretical developments and simulation results are provided.

I. Introduction

In a recent work this author suggested an approach that is based on nonlinear anisotropic damping forces (NADF) [1] to enable a harmonic potential field (HPF) motion planner [2-4] to generate an intelligent control signal capable of yielding a dynamic trajectory that preserves all the properties guaranteed by its kinematic counterpart. The NADF approach demonstrated better performance compared to popular approaches such as Guldner and Utkin sliding mode approach [5] and direct augmentation of the HPF gradient field ($-\nabla V$) with viscous damping to generate the control signal (u) [6]

$$u = -B\cdot \dot{x} - \nabla V(x) \quad . \tag{1}$$

It ought to be mentioned that in both approaches preserving the collision avoidance property guaranteed by the kinematic HPF planner is a concern.

This work provides two extensions of the NADF approach. The first is a blind, iterative procedure that enables the approach to handle systems with drift. The method based on clamping control suggested in [1] to handle the presence of external forces can only reduce the error to an arbitrarily small value. On the other hand, the suggested iterative procedure can totally cancel the steady state error. The other extension has to do with adapting the NADF approach to work with nonholonomic systems.

This paper is organized as follows: section II provides a brief background of the HPF approach. The NADF approach is quickly presented in section III. Sections IV and V discuss the application of the approach to dissipative systems and systems experiencing external forces respectively. Section VI deals with the extension to the nonholomic case. Simulation results are in section VII, and conclusions are placed in section VIII.

II. Background

Although the HPF approach was brought to the forefront of motion planning independently and simultaneously by different researchers [7-9], the first work to be published on the subject was that by Sato in 1986 [7]. The HPF approach forces the differential properties of the potential field to satisfy the Laplace equation inside the workspace of a robot (Ω) while constraining the properties of the potential at the boundary of Ω ($\Gamma=\partial\Omega$). The boundary set Γ includes both the boundaries of the forbidden zones (O) and the target point (x_T). A basic setting of the HPF approach is:

$$\nabla^2 V(x) \equiv 0 \qquad x\in\Omega$$
$$\text{subject to:} \quad V = 0|_{X=X_T} \;\&\; V = 1|_{X\in\Gamma} \quad . \tag{2}$$

The trajectory to the target (x(t)) is generated using the HPF-based, gradient dynamical system:

$$\dot{x} = -\nabla V(x) \qquad x(0) = x_0 \in \Omega \tag{3}$$

The trajectory is guaranteed to:

$$1-\ \lim_{t\to\infty} x(t) \to x_T \qquad 2-\ x(t)\in\Omega \qquad \forall t \tag{4}$$

whereby a proof of (4) may be found in [4]. Figure-1 shows the negative gradient field of a harmonic potential and the trajectory, x(t), generated using (3).

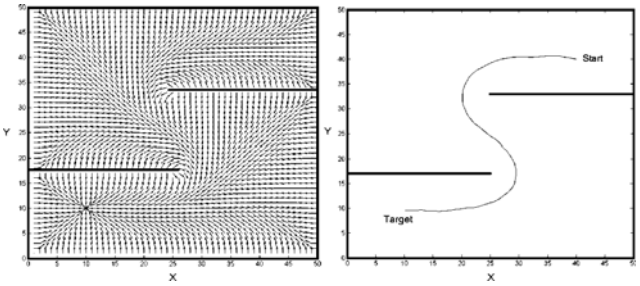

Figure-1: Guidance field and trajectory from an HPF.

III. The NADF Approach

The linear velocity component acts as a dampener of motion that may be used to place the inertial force under control by marginalizing its disruptive influence on the trajectory of the robot that the gradient field is attempting to generate. This approach ignores the dual role the gradient field plays as a control and guidance provider. A dampening component that is proportional to velocity exercises omni-directional attenuation of motion regardless of the direction along which it is heading. The guidance and disruptive components should not be treated equally. Attenuation should be restricted to the inertia-caused disruptive component of motion, while the component in conformity with the guidance of the artificial potential should be left unaffected.

A dampening component that treats the gradient of the artificial potential both as an actuator of dynamics and as a guiding signal is:

$$M(x,\dot{x}) = [(n^t \dot{\mathbf{x}})\, n + (\frac{\nabla V(x)^T}{|\nabla V(x)^T|} \cdot \dot{\mathbf{x}} \cdot \Phi(\nabla V(x)^T \dot{\mathbf{x}}))\frac{\nabla V(x)}{|\nabla V(x)|}] \quad (5)$$

where **n** is a unit vector orthogonal to ∇V and **Φ** is the unit step function. This force is given the name: nonlinear, anisotropic, dampening force (NADF).

IV- Dissipative Systems

In this section two propositions are stated for dissipative systems. Proofs may be found in [1].

Proposition-1: Let V(x) be a harmonic potential generated using the BVP in (2). The trajectory of the dynamical system:

$$\mathbf{D}(\mathbf{x})\ddot{\mathbf{x}} + \mathbf{C}(\mathbf{x},\dot{\mathbf{x}})\dot{\mathbf{x}} + \mathbf{B}_d \cdot \mathbf{M}(\mathbf{x},\dot{\mathbf{x}}) + \mathbf{K} \cdot \nabla \mathbf{V}(\mathbf{x}) = \mathbf{0} \quad (6)$$

will globally, asymptotically converge to:

$$\lim_{t\to\infty} \mathbf{x} \to \mathbf{x_T}, \quad \lim_{t\to\infty} \dot{\mathbf{x}} \to \mathbf{0}$$

for any positive constants B_d and K, where $x \in R^N$, $V(x): R^N \to R$, $D(x)$ is an $N \times N$ positive definite inertia matrix, $C(x,\dot{x})\dot{x}$ contains the centripetal, Coriolis, and gyroscopic forces. For a proof of the preposition see [1].

Proposition-2: Let ρ be the trajectory constructed as the spatial projection of the solution, x(t), of the first order differential system in (3). Also Let ρ_d be the trajectory constructed as the spatial projection of the solution, x(t), of the second order system in (6), figure-2. Then there exist a Bd that can make the maximum deviation between ρ and ρ_d (δ_m) arbitrarily small. For a proof of the preposition see [1].

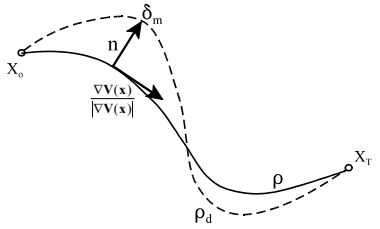

Figure-2: The kinematic and dynamic trajectories.

V. Systems with External Forces

The NADF approach may be adapted for designing constrained motion controller for mechanical systems experiencing external forces (e.g. gravity). The dynamical equation of such systems has the form:

$$D(x)\ddot{x} + C(x,\dot{x})\dot{x} + G(x) = F \quad (7)$$

where G(x) and F are vectors containing the external forces and the applied control forces respectively. The controller:

$$F = -B_d \cdot M(x,\dot{x}) - K \cdot \nabla V(x). \quad (8)$$

has the ability to make the trajectory of the system in (7) closely follow the kinematic trajectory from an initial starting point (x_o) to the target point x_T. However, due to the presence of the external forces the controller will not be able to hold the state close to the target point and drift will occur (Figure-10). Here an approach for effectively dealing with this type of systems is suggested.

1. Clamping control:

The effect of the clamping control (F_c) is strictly localized to a hyper sphere of radius σ surrounding the target point. If motion is heading towards the target, this control component is inactive. On the other hand, if motion starts heading away from the target, the control becomes active and attempts to drive the trajectory back to the target (Figure-3). A form of a clamping control that behaves in the above manner is:

$$F_C(x,\dot{x}) = (x - x_T) \cdot \Phi(\sigma - |x - x_T|) \cdot \Phi(\dot{x}^T(x - x_T)) \quad (9)$$

The strength of F_c is adjusted using the constant K_c so that the steady state error is kept below a desired level (ϵ). Clamping control maintains stability for any positive K_c.

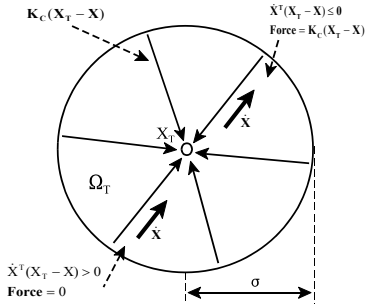

Figure-3: The clamping control.

Proposition-3:

For the mechanical system in (7), a controller of the form:

$$F = -B_d \cdot M(x,\dot{x}) - K \cdot \nabla V(x) - K_C \cdot F_C(\dot{x},x) \quad (10)$$

can make $\lim_{t\to\infty} |x(t) - x_T| \le \varepsilon < \sigma$ and $\lim_{t\to\infty} \dot{x} = 0$ (11)

provided that:

1- K, B_d, and K_c are all positive,

2- $K_c \ge F_{max}/\epsilon$, $F_{max} = \max_X |G(x)|$ $x \in \Omega_\sigma$ & $\Omega_\sigma = \{x: |x - x_T| \le \sigma\}$. (12)

3- a high enough value of B_d is selected so that at some instant in time t` $|x(t`) - x_T| < \sigma$ (13)

4- K is high enough so that the gradient field is capable of directing the trajectory to Ω_σ

$$|K \cdot \nabla V(X)| > \left| G^T(X) \frac{\nabla V(X)}{|\nabla V(X)|} \right| \quad X \in \Omega - \Omega_\sigma \quad (14)$$

For a proof of the preposition see [1].

2. Iterative, blind error cancellation:

While clamping control has the ability to reduce the steady state error to an arbitrarily small value, sometimes it is desired that this error be totally cancelled. Here, an iterative, blind procedure is suggested for error cancellation. The procedure works by providing an alternative path (β) other than the error channel ($K_P \cdot e$, where K_P is a positive definite matrix) to supply the control signal (u) that is needed to hold the robot at a location x_T (figure-4),

$$u = k \cdot e + \beta \quad (15)$$

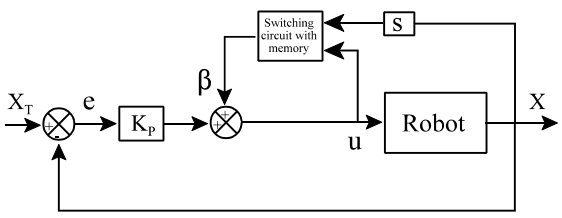

Figure-4: The suggested scheme for iterative error cancellation.

The fixed point iteration method [10] is used to evolve an estimate of the control signal so that the steady state error is driven to zero. This procedure is implemented using a switched logic circuit with one memory storage element. One implementation requires the circuit to have two inputs: the control that is directly fed to the robot and velocity of the robot's coordinates in order to assess convergence (other means to decide if the robot has converged may be used). There is only one output consisting of the bias term β. The bias term is iterativly determined as follows: when motion is about to settle (i.e. $|dx/dt| < \alpha$, where $0 < \alpha << 1$), the circuit measures the value of u and assigns it to β. This value is kept till at another instant i the event becomes true again. At the i'th instant we have:

$$u=G(x_i),\ \beta=G(x_{i-1}),\text{ and } K_P\cdot e = K_P\cdot(x_T-x_i) \quad (16)$$

where x_i is the position of the robot at the i'th settling instant. Relating the above quantities using (15) yields the recursive relation:

$$G(x_i) = G(x_{i-1}) + K_P\cdot(x_T-x_i)\ . \quad (17)$$

Proposition-4:

The recursive relation in (17) has a fixed point at which:

$$(x_T-x_i) = 0 \quad (18)$$

Proof: Using Taylor series expansion around x_T, we have:

$$G(x) = G(x_T) + J(G(x_T))(x-x_T)+ .... \quad (19)$$
$$= G(x_T) + F(x-x_T)$$

where J is the Jacobian matrix of G and F is a function containing the $(x-x_T)$ terms of the Taylor series. Substituting (19) into (17) we get:

$$F(e`_i) = F(e`_{i-1}) - K_P\cdot e`_i \quad (20)$$

where

$$e`_i = -(x_T - x_i)\ . \quad (21)$$

Now let $\eta=F(e`)$ and Q be the inverse function of F in the neighborhood of x_T. Substituting Q in (20), we obtain the recursive relation:

$$K_P\cdot Q(\eta_i) + \eta_i = \eta_{i-1}\ . \quad (22)$$

At a fixed point we have :

$$\eta_i = \eta_{i-1} \quad (23)$$

or

$$K_P\cdot Q(\eta_i) = 0.$$

Since K_P is positive definite, i.e. it is not singular:

$$Q(\eta_i) = e`_i = (x_i - x_T) = 0 \quad (24)$$

In other words:

$$x_i = x_T\ .$$

Proposition-5:

For any positive definite K_P, the fixed point $x=x_T$ is a stable attractor fixed point, i.e. if x_i is sufficiently close to x_T,

$$\lim_{i\to\infty} \mathbf{x_i} \to \mathbf{x_T} \quad (25)$$

Proof: In the close neighborhood of x_T, equation (17) may be written as:

$$J(G(x_T))\cdot(x_i-x_T) = J(G(x_T))\cdot(x_{i-1}-x_T) + K_P\cdot(x_T-x_i) \quad (26)$$

Notice that:

$$J(G(x_T)) = J(\nabla P(x_T)) = H(x_T) \quad (27)$$

where H is the symmetric hessian matrix. Substituting (27) in (26) yields the equation:

$$[K_P + H(x_T)]\cdot e_i = H(x_T)\cdot e_{i-1} \quad (28)$$

where

$$e_i = (x_T-x_i)\ .$$

Since K_P is positive definite and H is symmetric, they are simultaneously diagonalizable into:

$$K_p=UU^T \text{ and } H=U\Lambda U^T \quad (29)$$

where U is a nonsingular matrix and Λ is a diagonal matrix with non-negative elements λ_l, l=1,..,N, see [11, page-86].Using the above decomposition (28) may be written as:

$$U(I+\Lambda)U^T\cdot e_i = U\Lambda U^T\cdot e_{i-1} \quad (30)$$

Using the transformation $q_i = U^T\cdot e_i$,

we have

$$q_i = A\cdot q_{i-1} \quad (31)$$

where

$$\mathbf{A} = (\mathbf{I}+\Lambda)^{-1}\Lambda = \begin{bmatrix} \frac{\lambda_1}{1+\lambda_1} & 0 & \cdot & 0 \\ 0 & \frac{\lambda_2}{1+\lambda_2} & \cdot & 0 \\ \cdot & \cdot & \cdot & \cdot \\ 0 & 0 & \cdot & \frac{\lambda_N}{1+\lambda_N} \end{bmatrix}. \quad (32)$$

It is well-known that the solution of (31) is:

$$q_i = A^i\cdot q_0 \quad (33)$$

Since

$$0 \le \frac{\lambda_l}{1+\lambda_l} < 1 \qquad l=1,..,N \quad (34)$$

we have:

$$\lim_{i\to\infty} \mathbf{q_i} = \lim_{i\to\infty} \mathbf{U^T}\cdot\mathbf{e_i} \to \mathbf{0}\ . \quad (35)$$

Since U is a nonsingular matrix

$$\lim_{i\to\infty} \mathbf{e_i} \to \mathbf{0} \quad \text{or} \quad \lim_{i\to\infty} \mathbf{x}_i \to \mathbf{x_T} \quad (36)$$

VI. The Nonholonomic Case

In the following methods are outlined on how to adapt the HPF approach to work with nonholonomic robots to generate both kinematic and dynamic trajectories.

1. Kinematic, Nonholonomic, HPF-based planner:

The linearized equation of motion of a nonholonomic mobile robot may be written as:

$$\begin{bmatrix} \dot{\mathbf{x}} \\ \dot{\mathbf{y}} \\ \dot{\theta} \end{bmatrix} = \mathbf{H}(\mathbf{x},\mathbf{y},\theta)\begin{bmatrix} \nu \\ \omega \end{bmatrix} \quad (37)$$

where x and y are the coordinates of the center point of the robot, θ is its orientation, ν is the set radial speed of the robot, ω is the set angular speed, and H is a matrix function. The HPF approach may be directly applied to the robot in its linearized form by considering the set radial speed at a certain point in space to be equal to the magnitude of the gradient guidance field at that point and the set angular speed may be taken as the angle between the robot's orientation and the orientation of the gradient guidance field,

$$\nu = |-\nabla V(x,y)| \qquad \omega = \theta - \arg(-\nabla V(x,y)) \quad (38)$$

The above procedure can be with little effort adapted to many nonholonomic robots. However, in this work we are going to consider planning for a differential drive robot (figure-5).

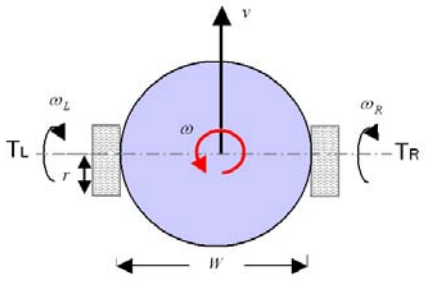

Figure-5: A differential drive mobile robot.

The equations describing motion for such a robot are:

$$\begin{bmatrix}\dot{\mathbf{x}}\\ \dot{\mathbf{y}}\\ \dot{\theta}\end{bmatrix}=\begin{bmatrix}\cos(\theta) & 0\\ \sin(\theta) & 0\\ 0 & 1\end{bmatrix}\begin{bmatrix}\nu\\ \omega\end{bmatrix} \tag{39}$$

and

$$\begin{bmatrix}\nu\\ \omega\end{bmatrix}=\begin{bmatrix}\frac{\mathbf{r}}{\mathbf{2}} & \frac{\mathbf{r}}{\mathbf{2}}\\ \frac{\mathbf{r}}{\mathbf{W}} & \frac{-\mathbf{r}}{\mathbf{W}}\end{bmatrix}\begin{bmatrix}\omega_R\\ \omega_L\end{bmatrix}=\mathbf{A}\begin{bmatrix}\omega_R\\ \omega_L\end{bmatrix} \tag{40}$$

where A is the dimension matrix of the robot, r is the radius of the robot's wheels, W is the width of the robot, ω_R and ω_L are the angular speeds of the right and left wheels of the robot respectively. The guidance signal derived from the HPF is:

$$\begin{bmatrix}\omega_R\\ \omega_L\end{bmatrix}=\mathbf{A}^{+}\begin{bmatrix}|-\nabla\mathbf{V}|\\ \theta-\mathbf{arg}(-\nabla\mathbf{V})\end{bmatrix} \tag{41}$$

where A^+ is the pseudo inverse of A. For a differential drive robot $A^+=A^{-1}$. The block diagram of the HPF planner for the kinematic case is shown in figure-6.

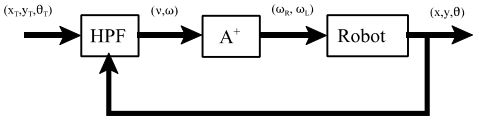

Figure-6: A Kinematic, HPF-based planner, Nonholonomic case.

The above scheme is tested for the gradient guidance field in figure-7. This field encodes the simple behavior of move right and stay at the center of the road (y=0).

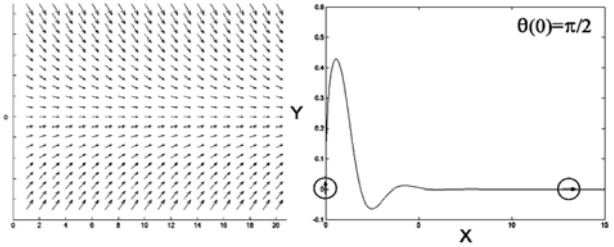

Figure-7: Move right and stay at center.

2. Dynamic, Nonholonomic, HPF-based planner:

The dynamic behavior of the differential drive robot that ties the torques applied to the right and left wheels (T_R, T_L) to the position and orientation of the robot may be described using two, coupled differential equations. The first one is obtained by differentiating equation-39 with respect to time,

$$\begin{bmatrix}\ddot{\mathbf{x}}\\ \ddot{\mathbf{y}}\\ \ddot{\theta}\end{bmatrix}=\begin{bmatrix}\cos(\theta) & 0\\ \sin(\theta) & 0\\ 0 & 1\end{bmatrix}\begin{bmatrix}\dot{\nu}\\ \dot{\omega}\end{bmatrix}+\begin{bmatrix}-\sin(\theta)\dot{\theta} & 0\\ \cos(\theta)\dot{\theta} & 0\\ 0 & 0\end{bmatrix}\begin{bmatrix}\nu\\ \omega\end{bmatrix}, \tag{42}$$

and the second is derived using Lagrange dynamics in the natural coordinates of the robot,

$$\begin{bmatrix}\dot{\nu}\\ \dot{\omega}\end{bmatrix}=\frac{\mathbf{1}}{\mathbf{M}}\begin{bmatrix}\frac{\mathbf{1}}{\mathbf{r}} & \frac{\mathbf{1}}{\mathbf{r}}\\ \frac{-\mathbf{4}\cdot\mathbf{r}}{\mathbf{W}^3} & \frac{\mathbf{4}\cdot\mathbf{r}}{\mathbf{W}^3}\end{bmatrix}\begin{bmatrix}\mathbf{T}_R\\ \mathbf{T}_L\end{bmatrix}=\mathbf{B}\cdot\begin{bmatrix}\mathbf{T}_R\\ \mathbf{T}_L\end{bmatrix} \tag{43}$$

where M is the mass of the robot. Choosing M=1, the dynamic model of the robot is used instead of the kinematic model in the example shown in figure-7 for the case of $\theta(0)=\pi/2$. As expected direct use of the guidance force as a control signal will fail (figure-8).

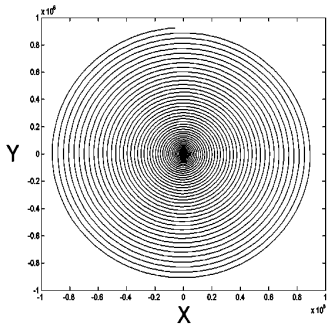

Figure-8: Adding mass causes instability.

To stabilize the system an omni-directional, linear viscous dampening force applied in the natural coordinates of the robot is used to generate the control signal:

$$\begin{bmatrix}\mathbf{T}_R\\ \mathbf{T}_L\end{bmatrix}=\mathbf{B}^{+}\cdot\left[\mathbf{K}_P\cdot\begin{bmatrix}|-\nabla\mathbf{V}|\\ \theta-\mathbf{arg}(-\nabla\mathbf{V})\end{bmatrix}-\mathbf{K}_d\cdot\begin{bmatrix}\dot{\rho}\\ \dot{\theta}\end{bmatrix}\right], \tag{44}$$

where K_P and K_D are positive constants, B^+ is the pseudo inverse of B, and $\dot{\rho}$ is the radial speed of the robot,

$$\dot{\rho}=\sqrt{\dot{\mathbf{x}}^2+\dot{\mathbf{y}}^2}\ . \tag{45}$$

The block diagram of the planner is shown in figure-9.

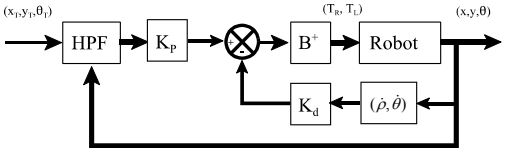

Figure-9: HPF-based planner with linear dampening, nonholonomic case.

The response of the system may be tuned using K_P and K_d. Significant transients should be expected for a small coefficient of rate feedback. Increasing this coefficient can reduce the transients, however, as in the holonomic case, it also reduces the speed of the robot.

One way to sensitize the dampening to the guidance signal is to notice that changing the speed of the robot is not needed if the actual speed of the system is equal to the reference speed. This leads to a simple, nevertheless effective, change in the form of the control signal:

$$\begin{bmatrix}\mathbf{T}_R\\ \mathbf{T}_L\end{bmatrix}=\mathbf{B}^{+}\cdot\left[\mathbf{K}_P\cdot\begin{bmatrix}|-\nabla\mathbf{V}|\\ 0\end{bmatrix}-\mathbf{K}_d\cdot\begin{bmatrix}\dot{\rho}\\ \dot{\theta}-(\theta-\mathbf{arg}(-\nabla\mathbf{V}))\end{bmatrix}\right] \tag{46}$$

The performance can still be further enhanced by making the reference radial speed at a certain point dependant on the orientation of the robot relative to the orientation of the guidance vector. The reasoning that may be used is: if the two orientations are the same use maximum reference speed. If the two orientations are at right angle use zero reference speed, and if the two orientations are diametrically opposite use a negative maximum reference speed. This reasoning may be implemented by simply multiplying the reference speed with cosine the difference between the two orientations. The control signal that realizes the above is:

$$\begin{bmatrix}\mathbf{T}_R\\ \mathbf{T}_L\end{bmatrix}=\mathbf{B}^{+}\cdot\left[\mathbf{K}_P\cdot\begin{bmatrix}|-\nabla\mathbf{V}|\cdot\cos(\theta-\mathbf{arg}(-\nabla\mathbf{V}))\\ 0\end{bmatrix}-\mathbf{K}_d\cdot\begin{bmatrix}\dot{\rho}\\ \dot{\theta}-(\theta-\mathbf{arg}(-\nabla\mathbf{V}))\end{bmatrix}\right] \tag{47}$$

VII. Results

A point mass with constant external forces having the system equation in (48) is controlled using the suggested approach,

$$\begin{bmatrix} \ddot{x} \\ \ddot{y} \end{bmatrix} = \begin{bmatrix} -4 \\ -4 \end{bmatrix} \tag{48}$$

As can be seen from figure-10, for a sufficiently high B_d the controller will succeed in driving the mass to the target and avoiding the obstacles. However, when the target is reached, drift caused by the external forces occur.

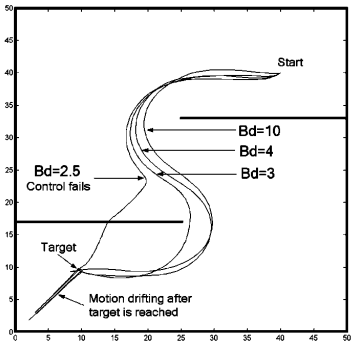

Figure-10: Trajectory, NADF - external force present.

In figure-11 a clamping control similar to the one in (9) is added with K=1, B_d=10, K_C=10. As can be seen, the controller was able to hold the trajectory near the target point relying only on a loose, upper bound estimate of the drift. Despite the high value of K_C , the trajectory settled in an overdamped manner with no oscillations taking place.

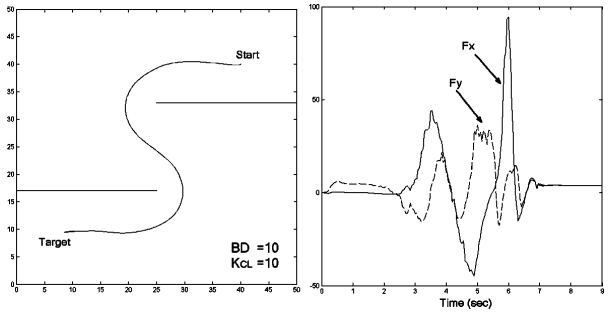

Figure-11: Trajectory and x-y control forces, NADF and clamping - external force present.

The iterative procedure to remove the steady state error suggested in section V is tested using a simple pendulum (figure-12) with concentrated mass M=1Kg and length L=1M. The dynamic equation of the pendulum is:

$$\mathbf{M} \cdot \mathbf{L} \cdot \ddot{\Theta} + \mathbf{M} \cdot \mathbf{g} \cdot \sin(\Theta) = \mathbf{u} \tag{49}$$

where g is the acceleration constant and u is the external applied control torque.

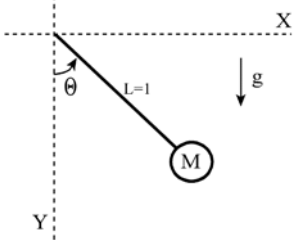

Figure-12: A simple pendulum.

A simple controller with position and velocity feedback (50) is used to move the pendulum from Θ=0 to Θ=π/2.

$$\mathbf{u} = -\mathbf{K} \cdot \Theta - \mathbf{B} \cdot \dot{\Theta} \tag{50}$$

As can be seen from figure-13, the weight of the pendulum causes significant steady state error. In order to remove the error, the switching circuit suggested in V.2 is added to the controller. Different switching thresholds are used to assess the sensitivity of the procedure to the presence of transients (figure-14). As can be seen, the error was eliminated in all cases. Although the iterative error cancellation procedure was designed to be used when transients fade away and motion settles, simulation shows that the procedure exhibits little sensitivity to the presence of transients that enables us to loosely choose the threshold α. Actually, the simulation reveals that better results in terms of having a lower settling time could be obtained if switching is carried out before motion completely settles.

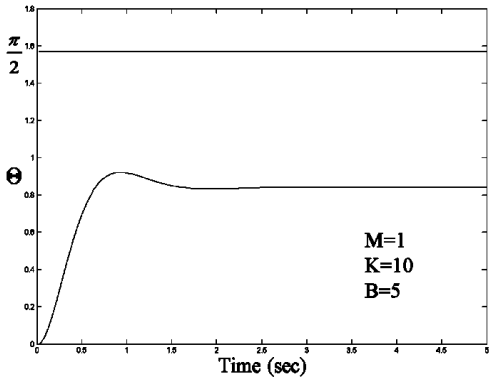

Figure-13: Steady state error caused by weight of pendulum.

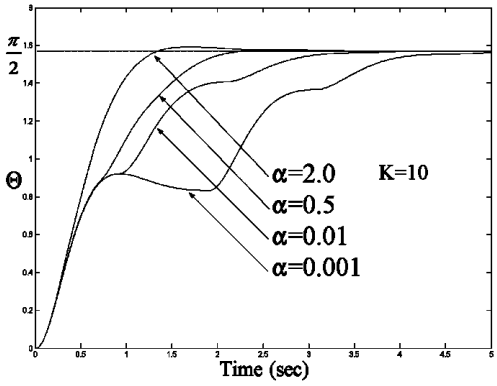

Figure-14: Error cancellation using switching circuit - different thresholds.

In figure-15 the PD control approach (44) in the natural coordinate of the nonholonomic robot is tested for different values of K_P and K_d. The two cases are simulated for the same duration. As can be seen, the use of rate feed back in the natural coordinates of the robot did stabilize the response and made the system yield to the guidance signal derived from the HPF. Significant transients are observed for a small coefficient of rate feedback. Although increasing this coefficient reduces the transients, it results, as in the holonomic case, in reducing the speed of the robot.

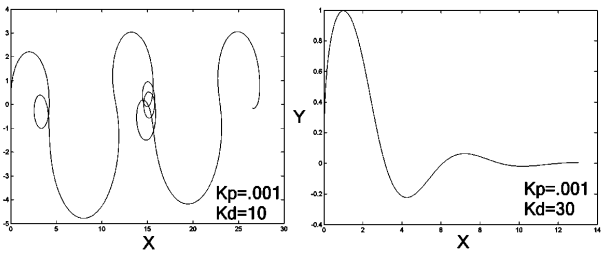

Figure-15: Response of the planner in (44) for different Kp and Kd.

In figure-16, the direction sensitive dampening is compared to the linear dampening case using same coefficients for the planner. As can be seen sensitizing the dampening to direction significantly reduced the overshoot and settling time without compromising the speed of the robot.

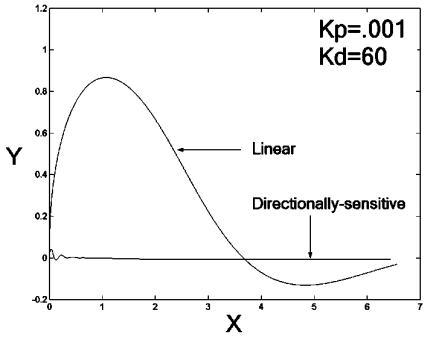

Figure-16: response of the planner in (46) compared to the one in (44).

In figure-17 the direction sensitive controller in (46) is compared to the jointly sensitized controller in (47). As can be seen the jointly sensitive controller lead to more reduction in the overshoot.

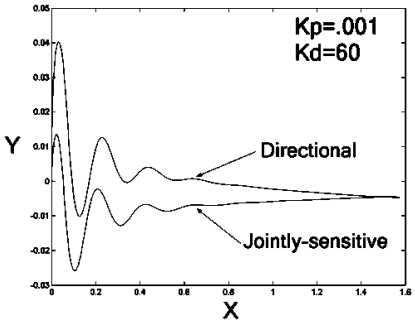

Figure-17: response of the planner in (46) compared to the one in (47).

Using a K_p=.001 and a K_d=60, The controller in (47) is tested in a cluttered environment. Figure-1 shows the harmonic gradient guidance field that is used to motivate the motion of the robot and the holonomic, kinematic trajectory such a field generates. Figure-18 shows the dynamic trajectory the controller generates and the orientation of the robot as a function of time. As can be seen, the nonholonomic, dynamic trajectory is very close in shape to the holonomic, kinematic trajectory with a satisfactorily smooth orientation profile. The control torques applied to the right and left wheels of the robot are shown in figure-19.

VII. Conclusions

In this paper the capabilities of the HPF approach are extended to tackle the kinodynamic planning case. The extension is based on a novel type of nonlinear, passive dampening forces called NADFs. The approach enjoys several attractive properties. It is easy to tune; it can generate a well-behaved control signal; the approach is flexible and may be applied in a variety of situations, it does not require exact knowledge of system dynamics, it can tackle dissipative systems as well as systems under the influence of external forces, and it can be extended to the nonholonomic case.

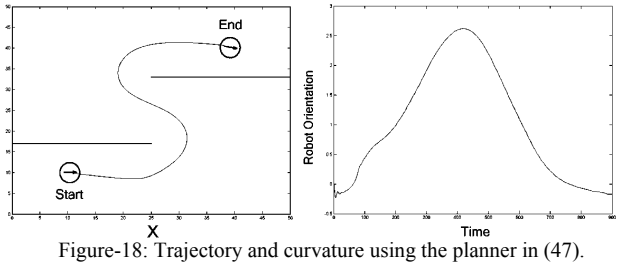

Figure-18: Trajectory and curvature using the planner in (47).

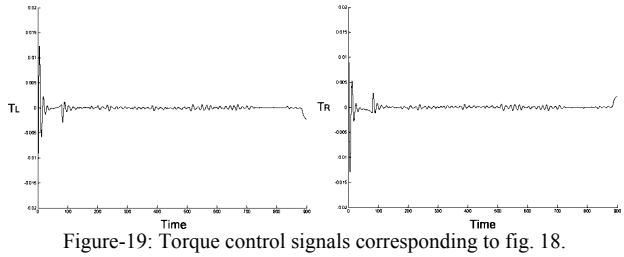

Figure-19: Torque control signals corresponding to fig. 18.

Acknowledgment

The author acknowledges KFUPM support of this work.

References

[1] Ahmad A. Masoud, "Agile, Steady Response of Intertial, Constrained, Holonomic Robots Using Nonlinear, Anisotropic Dampening Forces", Proceedings of the 45th IEEE Conference on Decision and Control, San Diego, CA USA, December 13-15, 2006, pp. 6167-6172.

[2] S. Masoud Ahmad A. Masoud, "Constrained Motion Control Using Vector Potential Fields", The IEEE Transactions on Systems, Man, and Cybernetics, Part A: Systems and Humans. May 2000, Vol. 30, No.3, pp.251-272.

[3] A. Masoud, Samer A. Masoud, Mohamed M. Bayoumi, "Robot Navigation Using a Pressure Generated Mechanical Stress Field, The Biharmonic Potential Approach", The 1994 IEEE International Conference on Robotics and Automation, May 8-13, 1994 San Diego, California, pp. 124-129.

[4] S. Masoud, Ahmad A. Masoud, " Motion Planning in the Presence of Directional and Obstacle Avoidance Constraints Using Nonlinear Anisotropic, Harmonic Potential Fields: A Physical Metaphor", IEEE Transactions on Systems, Man, & Cybernetics, Part A: systems and humans, Vol 32, No. 6, November 2002, pp. 705-723.

[5] J. Guldner, V. Utkin, "Sliding Mode Control for Gradient Tracking and Robot Navigation Using Artificial Potential Fields", IEEE Transactions on Robotics and Automation, Vol. 11, pp. 247-254, April 1995.

[6]D. Koditschek, E. Rimon, "Exact robot navigation using artificial potential functions," IEEE Trans. Robot. Automat., vol. 8, pp. 501–518, Oct. 1992.

[7] K. Sato, "Collision avoidance in multi-dimensional space using laplace potential," in Proc. 15th Conf. Robotics Soc. Jpn., 1987, pp. 155–156.

[8]C. Connolly, R.Weiss, and J. Burns, "Path planning using laplace equation," in Proc. IEEE Int. Conf. Robotics Automat., Cincinnati, OH, May 13–18, 1990, pp. 2102–2106.

[9]J. Decuyper and D. Keymeulen, "A reactive robot navigation system based on a fluid dynamics metaphor," in Proc. Parallel Problem Solving From Nature, First Workshop, H. Schwefel and R. Hartmanis, Eds., Dortmund, Germany, Oct. 1–3, 1990, pp. 356–362.

[10] V. I. Istratescu, "Fixed Point Theory, An Introduction", D.Reidel, Holland (1981). ISBN 90-277-1224-7

[11] H. Lutkepohl, "Handbook on Matrices", Wiley, 1996.